Available online at www.sciencedirect.com
SCIENCE DIRECT®
Journal of Nuclear Materials 337–339 (2005) 852–856
journal of nuclear materials
www.elsevier.com/locate/jnucmat

Plasma surface interaction with tungsten in ASDEX Upgrade

R. Dux *, A. Herrmann, A. Kallenbach, R. Neu, J. Neuhauser, H. Maier, R. Pugno, T. Pütterich, V. Rohde, ASDEX Upgrade Team

Max-Planck-Institut für Plasmaphysik, EURATOM Association, Boltzmannstr. 2-12, D-85748 Garching, Germany

Abstract

ASDEX Upgrade pursues the progressive increase of W coated plasma facing components. At present, the central column, the upper passive stabiliser loop, the complete upper divertor, the baffles at the lower divertor, as well as six tiles of one guard limiter at the low field side are W coated, representing about 65% of the total surface area. W erosion at these guard limiter tiles exceeds the erosion found at other main chamber components by more than one order of magnitude, and spectroscopically determined erosion yields indicate a strong contribution from fast particles. Upper single null discharges do not show an obviously increased W content compared to discharges run in the lower C based divertor.

PACS: 52.40.Hf; 52.25.Vy; 52.55.Fa
Keywords: First wall materials; Tungsten; Erosion; ASDEX Upgrade

1. Introduction

There is evidence that a future reactor will have to be designed as a full high-Z wall machine in order to provide long operation times [1]. Although W has a low erosion yield and a high sputtering threshold, its use implies the risk of unduly high radiation losses in the central plasma and concentrations above 10^{-4} would prevent ignition. Furthermore, the absence of carbon as a low temperature divertor radiator requires an active control of the radiated power with seed impurities.

ASDEX Upgrade is the only device, which employs tungsten as PFM on a large scale, following the route to a virtually carbon free device. After the successful operation with a full W divertor (W DivI) in 1995/1996 [2,3], a progressive increase of W PFCs in the main chamber has been pursued since 1999 [4]. For the 2003/2004 campaign, another 10.2 m^2 of W coated PFCs have been added to the already existing 14.6 m^2. Now, the central column, the upper passive stabiliser loop, the complete upper divertor as well as the baffles at the lower divertor are W coated, representing about 65% of the area of all PFCs. Additionally, one of the guard limiters at the low field side has been equipped with W coated tiles (Fig. 1). The new tiles were coated by plasma vapour deposition to a W thickness of 4 μm (instead of 1 μm used at the central column), to allow for the larger erosion fluxes expected in the upper divertor and at the guard limiter.

2. Operation with tungsten first wall and divertor

The W coatings were tested in thermal screening experiments up to melting conditions [5,6] and by cyclic

* Corresponding author. Tel.: +49 893 2991 256; fax: +49 893 2991 812.
E-mail address: rld@ipp.mpg.de (R. Dux).

0022-3115/$ - see front matter © 2004 Elsevier B.V. All rights reserved.
doi:10.1016/j.jnucmat.2004.10.105

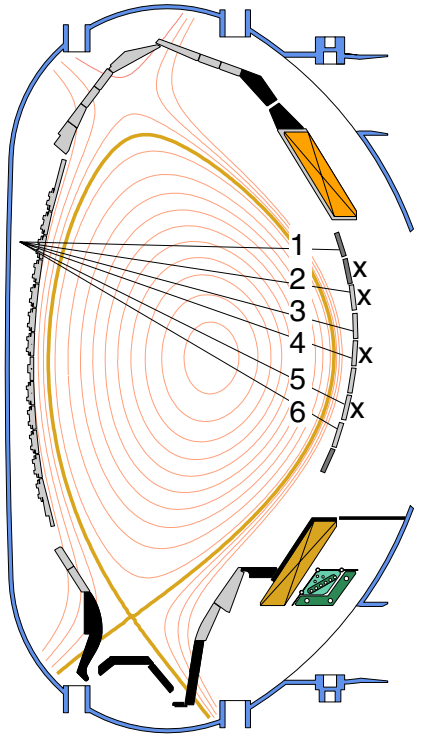

Fig. 1. In ASDEX Upgrade, about 65% of the area of all PFCs is presently coated with tungsten (grey). The lines-of-sight for W influx measurements from the limiter are shown, and the tiles, which are equipped with thermocouples, are indicated.

power loads, showing no failure under the specified conditions. However, during a recent vent it became evident, that a few of the newly installed W tiles exhibit delamination of the coating at the tile edges. Since this was also observed at regions with low or negligible power load, it was attributed to problems in the preparation or the production of the coating. Independently, melting of the W layer was found at tile edges in the strike point region of the upper divertor. In contrast to the arrangement chosen for W DivI, no tilting of the strikepoint tiles was applied in order to allow for an independent choice of I_p and B_t direction. As a consequence, the power load is up to a factor of 10 higher on the leading edge than on the flat surface.

Most of the experimental programme of ASDEX Upgrade could be performed without serious limitations resulting from tungsten contamination of the main plasma and the W concentration (c_W) usually stayed below a few $\times 10^{-5}$. Unlike with carbon PFCs, a strong difference between limiter and divertor operation is found and care has to be taken in designing the plasma shape in order to provide an adequate wall clearance. In discharges with peaked density profiles in combination with low diffusive transport, the central c_W could be reduced drastically by applying up to a few MW central RF wave heating [4,7]. ELM-free discharges or discharges with low ELM frequency, as are encountered at the H-L power threshold, showed increased c_W. These could be overcome by controlling the ELM frequency through pellet injection [8]. Special emphasis is devoted to the investigation of the influence of seeded impurities on the tungsten source since a future carbon-free device will crucially depend on radiatively cooled scenarios in order to mitigate the divertor power load. First experiments with argon seeding resulted in a significant reduction of the divertor electron temperature, while keeping the central density of W and Ar low [9] by applying central RF heating and ELM pace-making.

The discharges run so far with upper single null (USN) comprise ordinary L- and H-modes as well as plasmas with internal transport barrier. Discharges with low-power NBI beam heating show increased W concentrations, but in most scenarios, there is no obvious difference to discharges run in the lower (C based) divertor (LSN). Even during a continuous transition from USN to LSN no significant change in the W content could be identified. This is exemplified in Fig. 2. The upper two boxes of the figure show global plasma parameters together with H_α measured in the lower

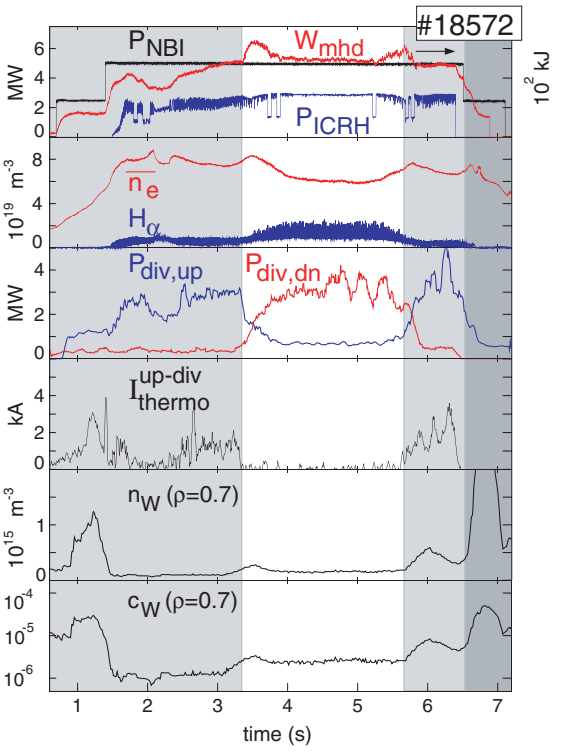

Fig. 2. Time traces for discharge #18572 with a continuous transition from USN (W coated tiles, light grey background) to LSN (C tiles) and back again. During ramp down at $t > 6.5$ s, the discharge is limited at the W coated central column.

divertor. After a short limiter phase until $t = 0.85$ s, the configuration is USN until about 3.3 s followed by a LSN phase of 1.4 s. Backtransition to USN occurs at 5.7 s, and finally, the discharge is terminated in a limiter configuration at the W coated central column for $t > 6.5$ s. The transition between USN and LSN is clearly visible in the power flowing to the corresponding divertor $P_{\mathrm{div,up}}$ and $P_{\mathrm{div,dn}}$. The thermo current $I_{\mathrm{thermo}}^{\mathrm{up-div}}$ is measured in the upper inner divertor. It is roughly proportional to the electron temperature T_e of the divertor plasma [9]. The two lowest time traces illustrate the temporal behaviour of the tungsten density n_W and concentration c_W in the main plasma deduced from spectroscopy [4]. The W-concentration is very low throughout the flattop phase of the discharge, and n_W is very similar in both divertor phases. The increase of n_W at 1.3 s and 6.0 s may be partly attributed to higher divertor T_e. The change of the confinement for the different divertors can be attributed to the different H-mode thresholds for opposite $B \times \nabla B$ drift directions with respect to the X-point location, which leads to different ELM regimes as already observed with a graphite upper divertor [10]. It should be noted that the discharge which resulted in melting of the leading edges in the upper divertor occurred before the discharge discussed here.

3. Tungsten erosion at the guard limiter

ASDEX Upgrade has 12 poloidal limiters on the low field side: a pair of side limiters for each of the 4 ICRH antennas and a pair of guard limiters at each side of the 2 neutral beam ducts, which are between the two ICRH antenna doublets. In radial direction, the 4 guard limiters are about 12 mm behind the ICRH antennas at the present time. One guard limiter was equipped with 6 tungsten coated tiles. After 330 discharges, the W erosion on one tile was measured post-mortem by X-ray fluorescence analysis. Depending on the position on the tile an erosion of up to 1.2 μm was detected. This represents an erosion rate of about a factor of 30 above the maximum value found at other main chamber components [11]. At the same time, no signs of melting, arcs, or delamination were found.

The larger erosion at the limiter allowed for spectroscopic tungsten influx measurements and 5 lines-of-sight detectors were installed to observe the tungsten tiles. The spots have a diameter of ≈2.5 cm and cover that part of the tile which has minimum distance to the plasma. Tungsten influx was monitored by measuring WI line radiation at 400.8 nm. The Balmer-δ transition at 410.1 nm was used to calculate the deuterium influx. The measured photon fluxes were transformed into ion fluxes using the number of ionisations per emitted photon, i.e., the (S/XB) value. For tungsten (S/XB) = 20 was used [12], and for H_δ, the atomic value (S/XB) = 3.3×10^3 was multiplied by a factor of 1.5 as a rough estimate for the molecular flux contribution [13]. The detection limit for W influx was at $\approx 2 \times 10^{17}\,\mathrm{m^{-2}s^{-1}}$.

The measured W influx densities Γ_W show a wide variation from below the detection limit to values of $\Gamma_W \approx 10^{19}\,\mathrm{m^{-2}s^{-1}}$. For ohmically and ECR heated discharges, the tungsten influx is below or close to the detection limit and higher values are only observed in plasmas with ICRH or NBI heating. Transiently, even higher values of $\Gamma_W = 8 \times 10^{19}\,\mathrm{m^{-2}s^{-1}}$ occur, when the separatrix is very close to the limiter. Thus, Γ_W reaches similar values as in W DivI, where influxes up to $4 \times 10^{19}\,\mathrm{m^{-2}s^{-1}}$ were measured [12]. It has a strong dependence on the distance between the position on the limiter and the separatrix, x. The co-ordinate x is the radial distance of the flux surface through the limiter position to the separatrix measured at the outboard side on a horizontal plane through the magnetic axis. The flux can roughly be described with $\Gamma_W \propto \exp(-x/\lambda)$ with $\lambda = 1.5$ cm. This can be seen from Fig. 3, where the logarithm of the flux ratio of either two channels are shown versus the scaled difference of separatrix distances $\Delta x/\lambda$. Measured power decay lengths are ≈4 cm in the SOL and ≈8 mm in the limiter shadow [14], while the influx decay length is a mixture of both situations, since the guard limiter is usually only partly in the shadow of the ICRH limiters.

Erosion yields were calculated by dividing Γ_W by the deuterium flux Γ_D. The heavy tungsten atoms radiate very close to the limiter and the spectroscopic measurement yields the local erosion flux at the observed spot.

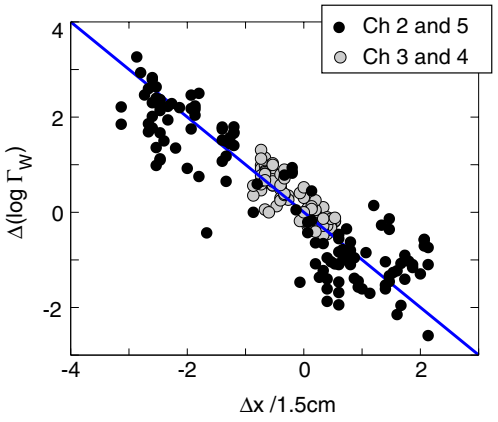

Fig. 3. The logarithm of the ratio of the W influxes from two limiter positions are plotted versus the difference of the radial distances to the separatrix Δx. Negative values of Δx are obtained from plasmas with less wall clearance on the upper part of the limiter and positive values represent less clearance at the lower part as in Fig. 1. The spatial dependence is roughly $\Gamma_W \propto \exp(-x/\lambda)$ with $\lambda = 1.5$ cm (solid line).

Deuterium, which starts inside the spot, can travel a longer path before being ionised and the photon emitting deuterium cloud has a considerably larger extent than the observed spot. The size of the photon emitting cloud was estimated by comparing the photon fluxes of spot measurement and measurement with a large observation window of 11.5 cm size in toroidal and 30 cm in poloidal direction, which encloses the spot position. The window measurement had on average a factor of 2.3 lower photon flux density. Neglecting poloidal variations inside the window, this ratio is explained by a 5 cm (11.5 cm/2.3) wide emission cloud. Thus, the photon flux density was multiplied by a factor of 2, i.e., the ratio of the widths of the emission cloud and spot size, where poloidal homogeneity of the hydrogen influx on the 5 cm scale is assumed, such that the poloidal dimension of the emission cloud drops out.

The quantity $Y_{\mathrm{eff}} = \Gamma_{\mathrm{W}}/\Gamma_{\mathrm{D}}$ is an effective value, and includes the sputtering by deuterium as well as by plasma impurities like carbon and oxygen. It varies from below 10^{-5} to about 2×10^{-3}, and approaches 10^{-2} for transient phases. For the interpretation of these values, a knowledge of the energy spectrum of the incident ions is needed. Three tungsten tiles are equipped with a thermocouple, which yields the deposited energy on the tile during the whole discharge. Discharges with little variations of heating power, plasma density and magnetic geometry were selected, such that the deposited energy is a good representative of the average power flux onto the tile. The deposited energy due to plasma radiation was considered and yielded at maximum a 25% correction. The deuterium flux onto the tile was calculated by multiplying the flux densities by the 10 cm height of the tile and the 5 cm width of the emission cloud. Thus, we arrive at an average deposited energy per deuterium ion, $E^{\mathrm{D}}_{\mathrm{dep}}$. It includes the deposited energy due to all plasma species, including the recombination energies, and is just an average value, while the sputtering yield is a strongly non-linear function of the kinetic ion energy. Fig. 4 shows Y_{eff} versus $E^{\mathrm{D}}_{\mathrm{dep}}$. The uncertainty estimate is indicated as being a factor of 2 for $E^{\mathrm{D}}_{\mathrm{dep}}$ and a factor of 4 for Y_{eff}. Y_{eff} varies by about two orders of magnitude for a change of $E^{\mathrm{D}}_{\mathrm{dep}}$ of about a factor of 20.

Some theoretical estimates based on the physical sputtering yields of tungsten as given in [15,16] are also shown in Fig. 4. The solid curve is calculated, assuming a thermal plasma with different edge temperatures and an ion flux of D^+ with an admixture of 1% C^{4+}. The kinetic ion energy was taken as $(2 + 3Z)\ k_{\mathrm{B}}T$ and for the deposited energy, the recombination energies and 2 $k_{\mathrm{B}}T$ for the electrons were added. The dominant sputtering contribution is due to carbon and the effective yields were taken from Ref. [17], which also take into account the deposition and erosion (physical and chemical) of carbon on the surface and its influence on the tungsten erosion. These non-linear effects are weak for the high

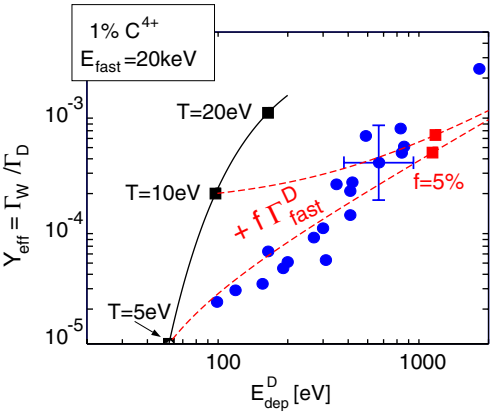

Fig. 4. Measured effective erosion yields of tungsten are shown versus the average deposited energy per D ion (blue dots). Calculated yields are plotted for the case of a thermal plasma with carbon dominated sputtering assuming a C^{4+} flux contribution of 1% (solid line), and for the case of fast D^+ ion dominated sputtering with fast ions of 20 keV energy for two fixed edge temperatures of 5 eV and 10 eV. The fast D^+ ion fraction increases along the dashed lines and reaches 5% of the total D^+ flux at the red squares. (For interpretation of the references in colour in this figure legend, the reader is referred to the web version of this article.)

T_e values and reduce the erosion yield by a factor of 2 for T_e = 5 eV. The obtained yields can explain the whole range of measured values, however, the deposited energy is much too low. The high values of $E^{\mathrm{D}}_{\mathrm{dep}}$ can only be explained by fast ions from NBI or ICRH heating. Detailed calculations of the fast particle load on the limiter have started. Here, the effect is just exemplified by using a fixed fast ion energy E_{fast} of 20 keV with a variable fraction of fast deuterium ions to the total impinging ion flux at two fixed plasma edge temperature of 5 eV and 10 eV (dashed lines in Fig. 4). The measured erosion yields are also covered and $E^{\mathrm{D}}_{\mathrm{dep}}$ is consistent with the experimental data, which can only be explained by a considerable fraction of fast particles.

4. Conclusion

The increase of the tungsten coated areas in ASDEX Upgrade to about 65% of all PFCs has not lead to seriously high tungsten concentrations, which can easily be kept below 10^{-5}. This holds for diverted discharges, where usage of the upper W divertor or the lower graphite divertor does not yield obvious differences, while limiter discharges at the central column have higher c_{W} values. In diverted H-mode discharges, central W concentrations are mainly determined by impurity transport in the plasma centre or in the H-mode barrier and can be

controlled by applying central wave heating and/or ELM pace making.

Tungsten erosion fluxes at the guard limiter are sufficiently strong to be measured spectroscopically. At the positions with the highest load, the campaign averaged erosion rate is by more than one order of magnitude higher than at other main chamber components. The local tungsten influx reaches similar values as previously measured in W DivI with a strong dependence on the distance to the separatrix. The measured effective erosion yields are quite high and could be explained by carbon dominated sputtering with plasma edge temperatures of $\approx 5-25$ eV. However, the measured mean ion energies point towards a dominant fast D^+ particle contribution to the sputtering of tungsten.

References

[1] H. Bolt, V. Barabash, G. Federici, et al., J. Nucl. Mater. 307–311 (2002) 43.
[2] R. Neu, K. Asmussen, K. Krieger, et al., Plasma Phys. Control. Fus. 38 (1996) A165.
[3] K. Krieger, H. Maier, R. Neu, ASDEX Upgrade Team, J. Nucl. Mater. 266–269 (1999) 207.
[4] R. Neu, V. Rohde, A. Geier, et al., J. Nucl. Mater. 313–316 (2003) 118.
[5] H. Maier, J. Luthin, M. Balden, et al., Surf. Coating Technol. 142–144 (2001) 733.
[6] H. Maier, J. Luthin, M. Balden, et al., J. Nucl. Mater. 307–311 (2002) 116.
[7] R. Dux, R. Neu, A.G. Peeters, et al., Plasma Phys. Control. Fus. 45 (2003) 1815.
[8] R. Neu et al., 30th EPS Conference, St. Petersburg, vol. 27A, EPS, Geneva, 2003, p. P1. 123.
[9] A. Kallenbach et al., these Proceedings, doi:10.1016/j.jnumat.2004.10.027.
[10] A. Herrmann, A. Carlson, J.C. Fuchs, et al., J. Nucl. Mater. 290–293 (2001) 619.
[11] H. Maier, ASDEX Upgrade Team, J. Nucl. Mater. 335 (2004) 515.
[12] A. Thoma, K. Asmussen, R. Dux, et al., Plasma Phys. Control. Fus. 39 (1997) 1487.
[13] H.P. Summers, Tech. Report JET-IR 06, JET Joint Undertaking, Abingdon, UK, 1994.
[14] A. Herrmann et al., these Proceedings, doi:10.1016/j.jnumat.2004.10.126.
[15] W. Eckstein et al., Tech. Report IPP 9/82, MPI für Plasmaphysik, Garching, Germany, 1993.
[16] W. Eckstein, Tech. Report IPP 9/132, MPI für Plasmaphysik, Garching, Germany, 2002.
[17] K. Schmid, J. Roth, J. Nucl. Mater. 313–316 (2003) 302.